Decision Tree Based Online Stability Assessment Scheme for Power Systems with Renewable Generations

Tong Wang, *Student Member, IEEE*, Tianshu Bi, *Member, CSEE, Senior Member, IEEE*, Haifeng Wang, *Senior Member, IEEE*, Jizhen Liu, *Member, CSEE, Member, IEEE*

***Abstract*—The stochastic fluctuation of renewable energy resources has significant impact on the stability of the power system with renewable generations and results in change in stability. Therefore, it is necessary to track the changing stability of the power system with renewable generations, a task that can be performed online. This paper details the use of decision trees to predict multi-mode damping of power system integrating renewable generations with the help of wide-area measurements system (WAMS). Power systems with renewable source generation are complex with vast amounts of data being collected from WAMS. Decision trees (DTs) are employed as a means to handle vast quantities of wide-area information, which involves the mode damping information indicating the stability. A 16-generator, 68-bus system with photovoltaic power generation and wind power generation is used as the test system. Remote signals obtained from phasor measurement units (PMUs) are employed as the input variables of DTs for predicting purposes. The simulation results demonstrate that the proposed predicting scheme is able to suggest the optimal course of action to remedy any near instability or unstable electromechanical oscillations even without prior knowledge of the varying output of the renewable source power.**

***Index Terms*—Decision tree, inter-area oscillations, mode damping, prediction, probabilistic density function, wide-area measurements.**

I. Introduction

THE low-frequency inter-area oscillations occurring in the frequency range of 0.1–2 Hz are inherent to the electric power system [1], [2]. However, when these oscillations get negatively damped and start affecting large groups of machines, they cause serious damage to the stability of the system. As such, investigating the impact of grid connection of large-scale centralized renewable source energy generation on existing power transmission systems is a vital issue. In particular, the random variation of renewable energy source generation at the level of the high-voltage transmission system, results in a greater emphasis on reliable and secure operations of power system incorporating renewable energy source generation. For secure system operation, it is, therefore, essential to accurately predict change in oscillation modes caused by variable renewable energy source power generation.

Grid-connected wind power and photovoltaic (PV) sources, which are being increasingly absorbed into conventional power systems, are attractive renewable energy options for large-scale applications. Connecting these sources to the grid has meant significant impact on power system dynamics and operational characteristics, including small-signal stability. Several studies investigating the impact of wind generation [3]–[6] and PV generation [7]–[9] on power system small-signal stability have concluded that the characteristic fluctuation of renewable energy resources is a critical factor influencing the stability of the power system. In particular, the high penetration of renewable energy resource generation changes the stability during the dynamic operational process. Currently, there are few studies that examine the online tracking of the changing stability of a power system that incorporates renewable energy source generation. Online tracking, an important decision tool for system operators, can suggest optimal remedial actions that can be taken for any near instability or unstable electromechanical oscillations in transmission networks. The development of this tool, therefore, is critical for an improved study of the small signal stability of power systems that incorporate renewable sources of generation.

Much work has been conducted in the area of damping factor estimation in large power systems to track the changing stability. In the past, the damping factor estimation methods have employed Eigen analysis [10], [11], Prony analysis [12], and Fourier based analysis [13] as the tool of stability assessment. Accurate damping factor estimation typically requires large amounts of data, which is why conventional damping factor estimation techniques are not suitable for rapidly detecting modal damping changes. Eigen analysis of the power system model provides an analytical approach for describing mode dynamics as well as for providing more insight into the cause and effect of poorly damped electromechanical modes [14]. However, model-based real-time identification of the instabili-

Manuscript received February 27, 2015; revised May 4 and May 21, 2015; accepted May 25, 2015. Date of publication June 30, 2015; date of current version May 31, 2015. This work was supported by the National Basic Research Program of China (973 Program) (No. 2012CB215206); National Natural Science Foundation of China (No. 51407071); the International Collaborative Project jointly Funded by the NSFC (No. 51311122), China, and the EPSRC, UK; Fundamental Research Funds for the Central Universities (No. 2014QN18) and China Postdoctoral Science Foundation (No. 2014M550683).

T. Wang (e-mail: hdwangtong@126.com), T. S. Bi, H. F. Wang and J. Z. Liu, are all with the State Key Laboratory of Alternate Electrical Power System with Renewable Energy Sources, North China Electric Power University, Beijing 102206, China.

Digital Object Identifier 10.17775/CSEEJPES.2015.00019

ty risk is still a challenge for power system operation. In fact, the models of the power system are never perfect and sometimes poorly damped modes may appear that are not reflected in the system model [15]. This trend is increasing due to higher penetrations of renewable energy sources generation with the characteristic of stochastic fluctuation, which are not properly reflected in the dynamic models.

The wide area measurement system (WAMS) enables the online identification of an accurate picture of dynamic states of a power system at a precise sample time [16], [17]. It provides important information for stability assessment and enhancement. The online stability method for predicting the security of large power systems include Fuzzy-logic based methods [18], [19], artificial neural networks [20], [21], and support vector machines [22], [23]. However, the most popular technique for online stability prediction for power systems today is the decision tree (DT) data mining technique [24]. Compared with other methods, DTs are simpler to build and easy to implement. By simulating large numbers of contingency cases off-line, a straight forward decision tree can be built for online stability assessment for traditional power systems [25]. In addition, there is a commercial tool for implementation of classification and regression tree (CART) developed by Salford Systems [26].

Typically, CART data is in the form of an array. In its simplest form, CART picks one measurement at a time for performing the splits, which is very effective in handling data having univariate attributes; however CART is difficult to use when the predictors are multivariate. In a large power system, there are multiple oscillations modes. One measurement alone cannot assess the stability accurately, which is why multiple measurements are necessary for online stability assessment. Therefore, it is necessary to develop a method to address multi-measurements in a single split. The algorithm described in this paper addresses multi-modal classifications by adding a pre-processing step in the input to the decision tree so as to represent high-dimensional data by a single variable.

A decision tree based stability assessment scheme is proposed in this paper to predict the mode damping, which can suggest to the operator the optimal course of action to remedy any near instability or unstable electromechanical oscillation. The remainder of this paper is organized as follows. Section II presents the probabilistic model of PV and wind power generation, respectively. In Section III, the proposed prediction scheme based on DTs is developed. The classification and regression tree is chosen as the algorithm of the decision tree. The classification trees are built using off-line data to achieve the classification rules. Regression trees using PMU data to be processed are then used to predict the mode damping of the power system incorporating renewable energy source generation. Section IV provides a test system with PV and wind power generation added. In Section V, remote signals obtained from PMUs are employed as input variables for prediction purposes; the simulation results demonstrate the effectiveness of the proposed prediction scheme. Section VI concludes this paper.

II. Probabilistic Model of Wind Power and PV Generation

A. The Probabilistic Model of Wind Power Generation

One of the most applicable probabilistic models of wind power generation is Weibull distribution, which describes the stochastic fluctuation of wind power generation. The probability distribution function (PDF) is shown in (1). $P_{\rm w}$ is the active power supplied by wind generation source connected to a multi-machine power system, $f_{\rm w}(\cdot)$ is the PDF of the wind power, $v_{\rm c}$ and $v_{\rm f}$ are the cut-in and furling wind speed, respectively. $F_{\rm w}(\cdot)$ is the cumulative distribution function (CDF) of Weibull distribution of wind speed, $\delta(P_{\rm w})$ is the impulse function, and $P_{\rm r}$ is the rated wind power.

$$f_{\rm w}(P_{\rm w}) = \begin{cases} \left[1-(F_{\rm w}(v_{\rm f})-F_{\rm w}(v_{\rm c}))\right]\delta(P_{\rm w}),\ (P_{\rm w}=0) \\ \dfrac{b}{d}\left(\dfrac{P_{\rm w}-h}{d}\right)^{b-1}\exp\left[-\left(\dfrac{P_{{\rm w}i}-h}{d}\right)^{b}\right],\ (0<P_{\rm w}<P_{\rm r}) \\ \left[F_{\rm w}(v_{\rm f})-F_{\rm w}(v_{\rm r})\right]\delta(P_{\rm w}-P_{\rm r}),\ (P_{\rm w}=P_{\rm r}) \\ 0,\ (P_{\rm w}<0 \text{ or } P_{\rm w}>P_{\rm r}). \end{cases} \tag{1}$$

Parameters in (1) are given by the following equations

$$\begin{aligned} b_i &= \left(\frac{\sigma_i}{\mu_i}\right)^{-1.086}, \quad d_i = \frac{P_{{\rm r}i}\mu_i}{(v_{{\rm r}i}-v_{{\rm c}i})\Gamma(1+1/b_i)} \\ h_i &= -\frac{P_{{\rm r}i}v_{ci}}{v_{{\rm r}i}-v_{{\rm c}i}}, \end{aligned} \tag{2}$$

where $\Gamma(\cdot)$ is a Gamma function, μ_i and σ_i are the mean and standard deviation of wind speed, respectively.

B. Probabilistic Model of PV Generation

The output power of photovoltaic station generation is related to the radiation intensity. Due to the stochastic fluctuation of the radiation intensity, the output of PV generation is also has the characteristic of stochastic fluctuation. Statistical results of large data demonstrate that the variable radiation intensity is distributed according to Beta distribution and the PDF is shown in (3)

$$f(E) = \frac{\Gamma(\alpha+\beta)}{\Gamma(\alpha)\Gamma(\beta)}\left(\frac{E}{E_{\max}}\right)^{\alpha-1}\left(1-\frac{E}{E_{\max}}\right)^{\beta-1}, \tag{3}$$

where E and $E_{\max}$ represent practical radiation intensity and maximum radiation intensity, respectively. The Beta distribution is a family of continuous probability distributions defined on the interval [0, 1] parameterized by two positive shape parameters, denoted by α and β, that appear as exponents of the random variable and control the shape of the distribution. The mean and covariance of Beta distribution are $\alpha/(\alpha+\beta)$ and $\alpha\beta/[(\alpha+\beta+1)(\alpha+\beta)^2]$, respectively.

The output power of a PV array is given by

$$P_{\rm pv} = EA\eta\eta_{\rm inv}, \tag{4}$$

where A represents the area of the array, η and $\eta_{\rm inv}$ represent the photoelectric conversion efficiency and efficiency of the grid-connected inverter. η is not a constant, and will change

with the radiation intensity E. The expression between η and E is given by

$$\eta = \begin{cases} \eta(E/E_k) & 0 \le E \le E_k \\ \eta & E > E_k, \end{cases} \tag{5}$$

where E_k represents the threshold value of radiation intensity. When the actual radiation intensity is less than the threshold value, the conversion efficiency linearly increases with radiation intensity. When the actual radiation intensity is beyond the threshold value, the conversion efficiency will remain constant.

From (5), it can be deduced that the output power of PV generation is also Beta-distributed. The output power of PV generation is also Beta-distributed as (6)

$$f(E) = \frac{\Gamma(\alpha+\beta)}{\Gamma(\alpha)\Gamma(\beta)} \left(\frac{P_{\rm pv}}{P_{\max}}\right)^{\alpha-1} \left(1 - \frac{P_{\rm pv}}{P_{\max}}\right)^{\beta-1}, \tag{6}$$

where $P_{\rm pv}$ and $P_{\max}$ represent the actual and maximum output power of PV generation, respectively.

By substituting (4) and (5) to (6), the PDF of the output power of PV generation is given by

$$f(P_{\rm pv}) = \begin{cases} \dfrac{\Gamma(\alpha+\beta)}{\Gamma(\alpha)\Gamma(\beta)} \left(\dfrac{E^2}{E_{\max}E_k}\right)^{\alpha-1} \left(1 - \dfrac{E^2}{E_{\max}E_k}\right)^{\beta-1} \\ (0 \le E \le E_k) \\ \dfrac{\Gamma(\alpha+\beta)}{\Gamma(\alpha)\Gamma(\beta)} \left(\dfrac{E}{E_{\max}}\right)^{\alpha-1} \left(1 - \dfrac{E}{E_{\max}}\right)^{\beta-1} \\ (E_k < E \le E_{\max}). \end{cases} \tag{7}$$

III. Decision Tree Based Prediction Scheme

A. Decision Tree

A decision tree is a flowchart-like structure in which each internal node represents a "test" on an attribute (e.g., whether a coin flip comes up heads or tails); each branch represents the outcome of the test and each terminal node represents a class label (decision taken after computing all attributes). The paths from root to terminal node represent classification rules.

Classification and regression tree [27] are non-parametric decision tree learning from a data set that produces either classification or regression trees. The classification tree is trained off-line and the regression tree is utilized online with real-time data. The branches of a decision tree end in a terminal node that denotes the different classes in which the data can be separated, with each observation getting mapped to its corresponding class. In this paper, each class represents the stability level, such as the mode damping of the power system. The basic design procedure involves five steps: 1) attribute selection, 2) data set generation, 3) tree growing, 4) tree pruning, and 5) performance evaluation.

B. Selection of Variables for Decision Tree

The guiding principle for the choice of variables is to select those system variables that are monitorable, controllable, and that adequately characterize an operating state of a power system from a classification point of view. C. M. Arora and Surana [28], [29] have shown that the real and reactive power generations of generators carry sufficient information about the class of system security. Meanwhile, since the oscillations manifest the active power oscillation between coherency groups, the tie-line flows between groups are considered as options. When multiple modes exist in the power system, only one tie-line flow is not adequate for classification. Thus, multiple tie-line flows between groups are considered as options. In this paper, the tie-line flows are chosen according to observability with respect to the oscillation modes. Moreover, tie-line flows in this paper are calculated using the angle shift δ_{ik} and the voltages provided by PMUs in real time, as shown in (8)

$$P_{ik} = \frac{U_i U_k}{X_{ik}} \sin(\delta_i - \delta_k) = \frac{U_i U_k}{X_{ik}} \sin \delta_{ik}. \tag{8}$$

In (8), δ_i and U_i are the angle and voltage magnitude of bus, while δ_k and U_k are the angle and voltage magnitude of bus, respectively.

C. Damping Classes

Before we proceed further, it is beneficial to qualify what constitutes a major deterioration in damping. Table I provides an assessment of damping performance as provided by the National Electricity Marketing Management Company Australia [30]. Based on the criteria in Table I, a change in damping will be considered unacceptable and detrimental if damping moves into the inadequate region (i.e., damping is worse than 0.07). In this manner, the damping classes are used as the terminal nodes of a decision tree of each oscillation mode.

TABLE I
QUALITATIVE REFERENCE TO DAMPING PERFORMANCE

Damping Ratio	Qualitative Description	Class
$\xi < 0$	Unstable	1
$0 < \xi < 0.05$	Very inadequate	2
$0.05 < \xi < 0.07$	Inadequate	3
$0.07 < \xi < 0.139$	Marginally adequate	4
$0.139 < \xi < 0.2$	Acceptable	5
$\xi > 0.2$	Highly acceptable	6

D. Tree Growing

The trajectory followed by the real power measurements corresponding to changes in the system parameters is used to predict the mode damping for stability assessment. Since a decision is being made based on a combination of the trajectories of different measurements, the Fisher's Linear Discriminant technique developed in [31] becomes a suitable choice for decision making. The distance from an optimally selected hyper-plane that is used for splitting two classes is given by

$$d = \left[\boldsymbol{h} - \frac{(\boldsymbol{\mu}_\alpha + \boldsymbol{\mu}_\beta)}{2}\right] (\boldsymbol{\Sigma}_\alpha + \boldsymbol{\Sigma}_\beta)^{-1} (\boldsymbol{\mu}_\alpha - \boldsymbol{\mu}_\beta)^{\rm T}. \tag{9}$$

In (9), d is the one-dimensional variable representing the distance to the hyper-plane that is sent to the classification tree for splitting purposes, $\boldsymbol{h}$ is the current operating point,

α and β are the two classes, respectively. $\boldsymbol{\Sigma}_\alpha$ and $\boldsymbol{\Sigma}_\beta$ are the covariances of the measurements of two classes α and β, respectively. $\boldsymbol{\mu}_\alpha$ and $\boldsymbol{\mu}_\beta$ are the means of the measurements of two classes α and β, respectively. According to the sign of the distance d, $\boldsymbol{h}$ is identified to be in class α or β. For example, if d is positive, the current operating point is identified to be in damping class α, and if d is negative, the current operating point is identified to be in damping class β. In this paper, the negative distance makes sense. Then, the regression tree is performed to learn where the current operating power system is and the class in which the current mode damping is. A new distance variable d' from the current operating point $\boldsymbol{h}'$ is dropped down to the decision tree, and the decision suggesting the current operating point is made upon reaching a terminal node, representing the damping ratio class. Finally, the damping class is adaptively determined by the terminal node.

On doing so, the distances from each point to the hyper-plane are then employed as the one-dimension input data for DT. For multiple measurements of multiple sampling points, the technique needs to be extended. Assume there exists damping classes, measurements for each damping class, and sampling points per second. Then, the original learning data set will be in a $n \times r$ dimensional space. Diverse disturbances around each sample are generated through a combination of output power of wind and PV generation scaling. This idea of performing diverse disturbance is to model the disturbances for guaranteeing the reliability of the identification method. Simulations with subsequently increasing and decreasing output power of wind and PV generation are carried out. If available, historical information of daily output power of wind and PV generation can further enhance the original data set.

By extending the idea into two dimension space developed to higher dimensions, the original data set into k subspaces can be separated such that each subspace contains the measurements belonging to one damping class. The hyper-planes that optimally partition the k damping class can then be expressed as $\boldsymbol{\pi}_{12}, \boldsymbol{\pi}_{13}, \cdots, \boldsymbol{\pi}_{ij}, \cdots, \boldsymbol{\pi}_{(k-1)k}$. The subscript of $\boldsymbol{\pi}_{ij}$ represent the i^{th} and j^{th} damping classes that partitioned optimally by the chosen hyper-plane. Due to Fisher's Linear Discriminant, the normal vector to the hyper-plane that maximizes separation of classes i and j is given by

$$\boldsymbol{m}_{ij} = \frac{(\boldsymbol{\Sigma}_i + \boldsymbol{\Sigma}_j)^{-1}(\boldsymbol{\mu}_i - \boldsymbol{\mu}_j)^{\mathrm{T}}}{\sqrt{(\boldsymbol{\mu}_i - \boldsymbol{\mu}_j)(\boldsymbol{\Sigma}_i + \boldsymbol{\Sigma}_j)^{-\mathrm{T}}(\boldsymbol{\Sigma}_i + \boldsymbol{\Sigma}_j)^{-1}(\boldsymbol{\mu}_i - \boldsymbol{\mu}_j)^{\mathrm{T}}}}, \tag{10}$$

where $\boldsymbol{m}_{ij}$ is $n \times 1$ unit normal vector of the hyper-plane. The distance between a point $\boldsymbol{h}(h_1, h_2, \cdots, h_i, \cdots, h_{n\times r})$ and the hyper-plane can be calculated by the projection, which the vector $\boldsymbol{h} - 1/2(\boldsymbol{\mu}_i + \boldsymbol{\mu}_j)$ projects on the unit normal vector $\boldsymbol{m}_{ij}$ given by (11).

$$d_{ij} = \left[\boldsymbol{h} - \frac{1}{2}(\boldsymbol{\mu}_i + \boldsymbol{\mu}_j)\right] \boldsymbol{m}_{ij}, \tag{11}$$

$$\begin{aligned}\boldsymbol{d} = [&d_{11} \cdots d_{1i} \cdots d_{r1} d_{21} \cdots d_{2i} \cdots d_{2r} \cdots \\ &d_{ij} \cdots d_{nj} \cdots d_{nr}], (0 \le i \le n, 0 \le j \le r).\end{aligned} \tag{12}$$

In this manner, the distance vector from one damping class to each hyper-plane is then calculated by (11) and (12). Meanwhile, the original data set in higher dimension space is reduced to the distance vector to the hyper-planes, which is one dimension. With prior knowledge of the distances of the data points from a previously computed hyper-plane, a decision tree is built.

Then, regression is performed to learn where the current damping class is in the parameter space. A new distance vector $\boldsymbol{d}'$ from current damping class $\boldsymbol{h}'$ to the hyper-plane $\boldsymbol{\pi}$ is dropped down the tree, and the decision to alter the current damping class is made upon reaching a terminal node. In this way, based on the PMU information trajectory in real time, DT is able to adaptively identify the current damping class. It then can suggest the optimal course of action to remedy any near instability or unstable electromechanical oscillations without prior knowledge of varying output of the renewable source power.

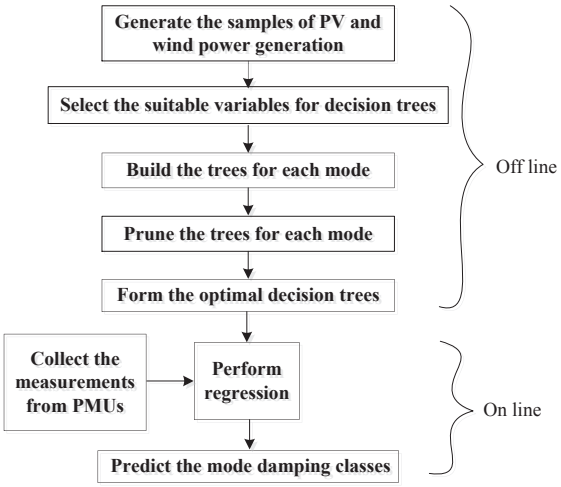

Fig. 1. Flowchart for DTs based on prediction scheme design procedure.

E. Tree Pruning

Pruning is the process of reducing a tree by turning some branch nodes into leaf nodes, and removing the leaf nodes under the original branch. Actually, pruning is basically an estimation problem. Since less reliable branches are removed, the pruned decision tree often gives better results over the whole instance space. Different pruning approaches use the testing data for pruning. However, pruning is necessary to improve the tree capability and reduce the error cost [27]. First, accuracy is computed by counting the misclassification at all tree nodes. Then, the tree is pruned by computing the estimates following the bottom-up approach (post-pruning). The cross-validation estimation is computed next. The cross-validation estimate provides an estimate of the pruning level needed to achieve the best tree size. Finally, the best tree is the one that has a residual variance that is no more than one standard error above the minimum values along the cross-validation line.

F. DT Based Prediction Scheme Design Procedure

Fig. 1 gives a flowchart of DT based prediction scheme design procedure. It is explained as follows.

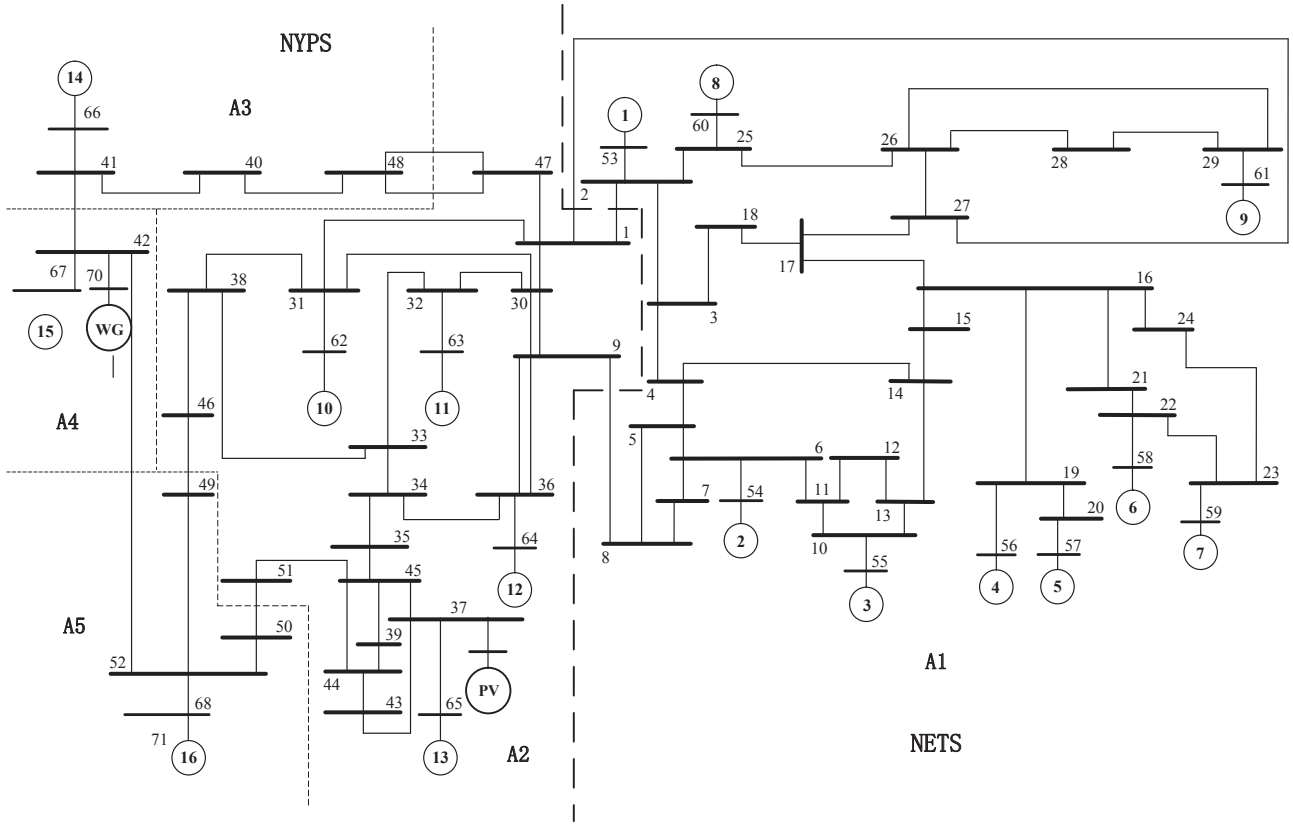

Fig. 2. The 16-generator, 68-bus test system added with PV and wind power generation.

Step 1: Generate the samples according to the PDF of PV and wind power generation. The samples are used to generate the trajectories as training data to train a tree.

Step 2: Select the suitable variables for DTs based on the highest observability of each oscillation mode.

Step 3: Grow DTs for each mode using the classification and regression tree as the algorithm.

Step 4: Prune DTs by cross-validation estimation.

Step 5: Form the optimum DTs for each mode.

Step 6: Collect the relative angles and calculate the real power flowing in the tie-lines. Send these wide-area signals to the optimal trees to perform regression.

Step 7: Predict the corresponding damping classes of each mode, and suggest to system operators the optimal course of action to remedy any near instability or unstable oscillations.

In this paper, the proposed method includes two stages, the off-line stage and the online stage. In the process of building the trees for each mode, Eigen analysis is used off-line, and the damping ratios with different samples of output power of wind and PV generation are classified to different damping classes in the first stage. In the second stage, the identification process, i.e., the regression is performed using wide area information to predict the mode damping classes online.

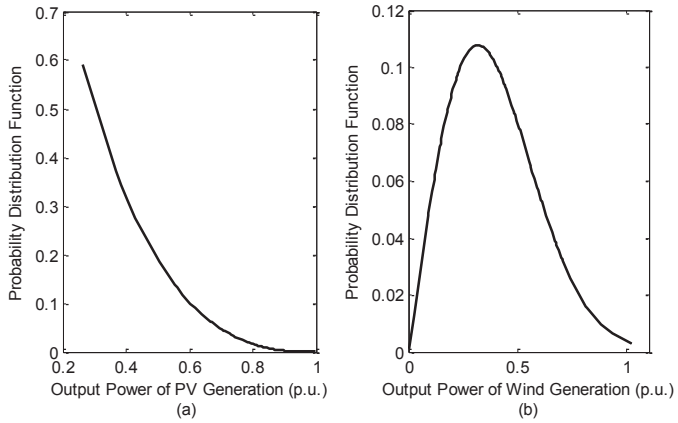

Fig. 3. The PDF of output power of PV and wind generation, respectively. (a) PV. (b) Wind generation.

IV. An Example Test System

A. Test System

A 16-generator, 68-bus system model of the New England-New York interconnected power system is used for testing the performance of the proposed method. A single line diagram of the system is shown in Fig. 2. The detailed values of this system can be found in [32]. IEEE type-1 DC excitation systems are installed in all the machines. The PV generation

station is added in bus 37, and wind power generation farm is added in bus 42.

The parameters of the wind speed distribution are as follows: $v_{\rm c} = 4$ m/s, $v_{\rm r} = 10$ m/s, $v_{\rm f} = 22$ m/s, $P_{\rm r} = 1.0$ p.u., $\mu = 8.2$, $\sigma = 2.5$.

The parameters of PV generation distribution are as follows: the maximum radiation intensity is $E_k = 150$ W/m^2, $E_{\max} = 2000$ W/m^2, the shape parameter is $\alpha = 2$, $\beta = 3.6$.

The PDFs of PV and wind power output are shown in Fig. 3. The x-axis represents the output of the PV and wind power generation in p.u., respectively. From Fig. 3, it can be observed that the small output power of PV generation is with higher probability, and the middle output power of wind generation is with higher probability, which agree with the natural phenomena. When the output power of wind and PV generation change, the power flow will change, along with the damping performance of the power system. The PDFs of four mode damping are shown in Fig. 4, in which it can be observed that the PDFs of the four mode damping ratios are not distributed according to standard Beta-distribution or standard Weibull distribution, due to the combination of different renewable energy resources according to different distributions. The y-axis demonstrates the probabilistic density function, and the whole area below the PDF curve is 1, which is the cumulative distribution function (CDF). The PDFs of the four modes in Fig. 4 are obtained through Monte Carlo simulation methods. The frequencies of Mode 1, Mode 2, Mode 3, and Mode 4 are around 0.28 Hz, 0.42 Hz, 0.64 Hz, and 0.77 Hz, respectively.

Table I gives the damping classes of decision tree. From Fig. 4, it can be seen that the minimum and maximum damping ratios of Mode 1 are about 0.03 and 0.08, respectively. Due to the damping classes shown in Table I, the damping ratios of Mode 1 can be classified into 3 damping classes, which are Class 2 (very inadequate), Class 3 (inadequate) and Class 4 (marginally adequate), while the damping ratios of modes 2, 3, and 4 are all classified to Class 2. Therefore, the other 3 modes except for Mode 1 are not necessary to build the decision tree for online stability assessment.

B. Formation of Decision Tree

The optimum variables as input of the decision tree are selected with the higher observability of active power with respect to Mode 1. The power flows of lines 1–2, 8–9, 41–42, and 50–51 are with the higher observability with respect to Mode 1. On the other hand, Mode 1 is the lowest frequency oscillation mode, with most generators participating. Therefore, the active power flow of the tie-lines between the five groups manifests the changes of Mode 1 the most.

The sample size of wind power generation is 100, and the sample size of PV generation is 100. The total number of samples is $100 \times 100 = 10,000$. And then, the sample rate of each of these 4 measurements are 30 points per second while the simulation is run for 1 second. For the present analysis, a total of 10,000 simulations were performed. Therefore, the complete learning sample for classification purposes consisted of 10,000 rows and 120 columns (30 points of 4 measurements).

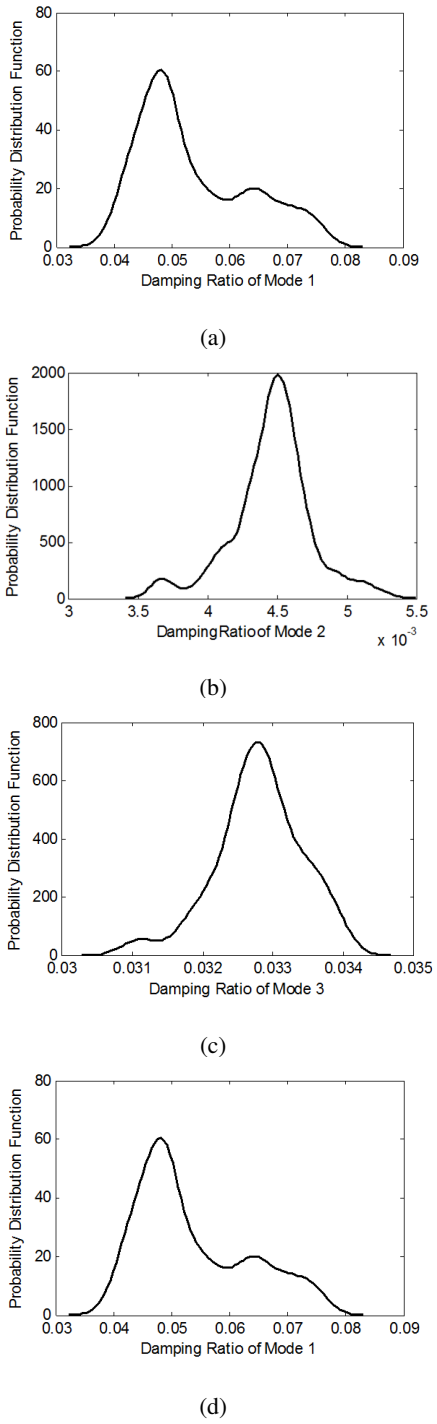

Fig. 4. The PDFs of 4 oscillation modes, respectively. (a) Mode 1. (b) Mode 2. (c) Mode 3. (d). Mode 4.

In this paper, the number of samples is 10,000, but in the real power system, the number of the samples is considerable. The larger the number of samples, the more accurate and effective the stability assessment is.

C. Optimal Tree for Prediction Purpose

In order to choose the optimal tree in terms of size and accuracy, a group of minimal cost-complexity sub-trees were analyzed as seen in Fig. 5. The selection of the tree size is made based on classification accuracy and tree complexity. A

tree with 11 terminal nodes was found to be suitable. The misclassification rate of that sub-tree is 16.85%.

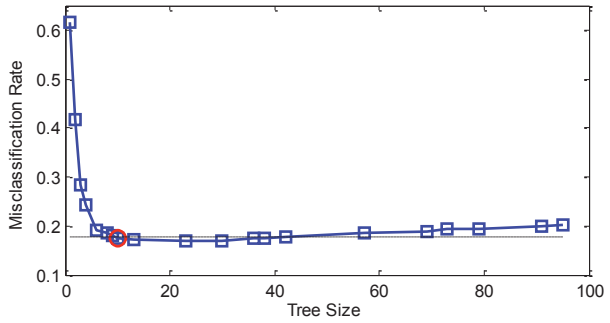

Fig. 5. Cross-validation estimate of the misclassification rate.

The selection of the tree size is made based on classification accuracy and tree complexity. In the process of disturbances generation, the measurement noises become involved, which may then influence the misclassification rate of the sub-tree.

In this paper, for each sample, disturbances are generated through a combination of wind and PV generation scaling. In the process of disturbance generation, the measurement noises are involved. In the test study, each combination of wind and PV generation increased by 10% or decreased by 10%. If the disturbances are set larger, the misclassification rate of the decision tree will increase. If the disturbances are set smaller, the misclassification rate of the decision tree will decrease.

The chosen sub-tree is shown in Fig. 6. It has 11 terminal nodes corresponding to the 3 classes, namely, damping classes 2, 3, and 4, respectively. The boxes with black frame represent the branches waiting to be split by the rule of distance vector to the hyper-planes. While the boxes with green, blue, and red frames represent the terminal nodes, which are not split any further, and demonstrate the results of the regression process. The red box denotes the damping Class 2; the green box denotes the damping Class 3; while the blue box denotes the damping Class 4. The distances from the operating point to the hyper-planes are expressed by d_1, d_2, and d_3.

The sampling rate is assumed to be 30 points per second. For example, in the first second, 120 measurements from P-MUs are sent to the decision tree. First, the 120 measurements represent the position in the 120 dimension hyper-space. Then, using (11), the distance vector to the three hyper-planes is calculated and dropped from the top to the bottom of the tree. As shown in Fig. 6, the splitting rule for the 1^{st} node is the distance to the 3^{rd} hyper-plane. If the distance to the 3^{rd} hyper-plane is bigger than -0.00026, then the distance vector arrives at node 3 for further splitting; if the distance to the 1^{st} hyper-plane is less than -0.00014, then the current damping class is identified to be Class 3 (Inadequate).

In this way, regression is performed using CART to know in which damping classes the current power system is in. The decisions to alter operators form the optimal course of action to remedy any near instability or unstable electromechanical oscillations.

V. Results and Analysis

To test the effectiveness of the proposed prediction method, the output sequence of PV generation is shown in Fig. 7(a), and the output sequence of wind power generation is shown in Fig. 7(b). The output power of wind and PV generation in three hours are assumed to be distributed according to Weibull and Beta-distribution, respectively. During the simulation process, the renewable energy resources are fluctuating as shown in Fig. 7. In this case, the measurements of tie-line flows are sent to the decision tree, as shown in Fig. 6, for regression and to make the decision about the stability state of the power system. The output trajectory of the decision tree is shown in Fig. 8. From Fig. 8, it can be seen that the minority is damping class 4, which is in accordance with that shown in Fig. 4. The red circles represent the prediction results using the decision tree online, and the blue dots represent the true damping classes using Eigen analysis.

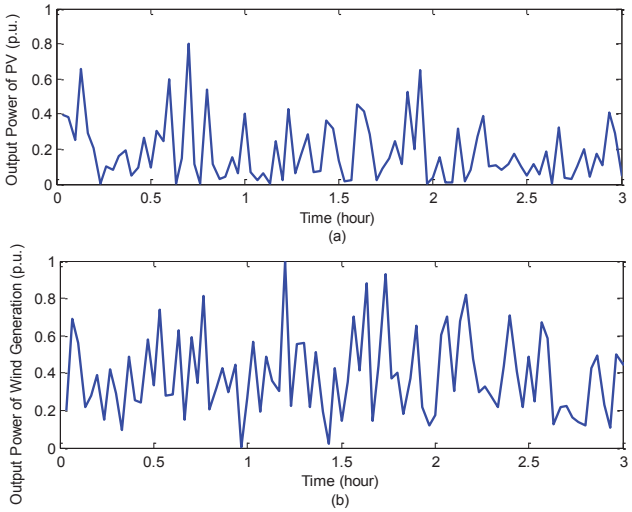

Fig. 7. The output sequences of PV and wind generations. (a) PV. (b) Wind generation.

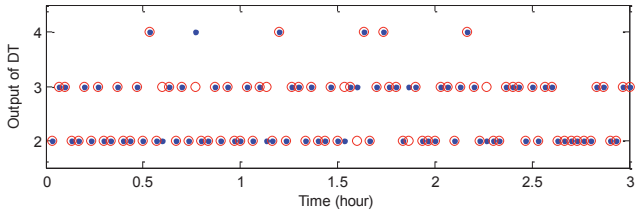

Fig. 8. The output trajectory of DT.

The output trajectory of DT of three hours is shown in Fig. 8, in which the results are the identification damping class of every two minutes. The total number of identification results is 90. Actually, the time interval of output of DT could be adjusted to 1 minute or other time intervals. From the 90 identification results with different output power of wind and PV generation, it can be seen that the identification results are accurate for the most part. Though the results of some

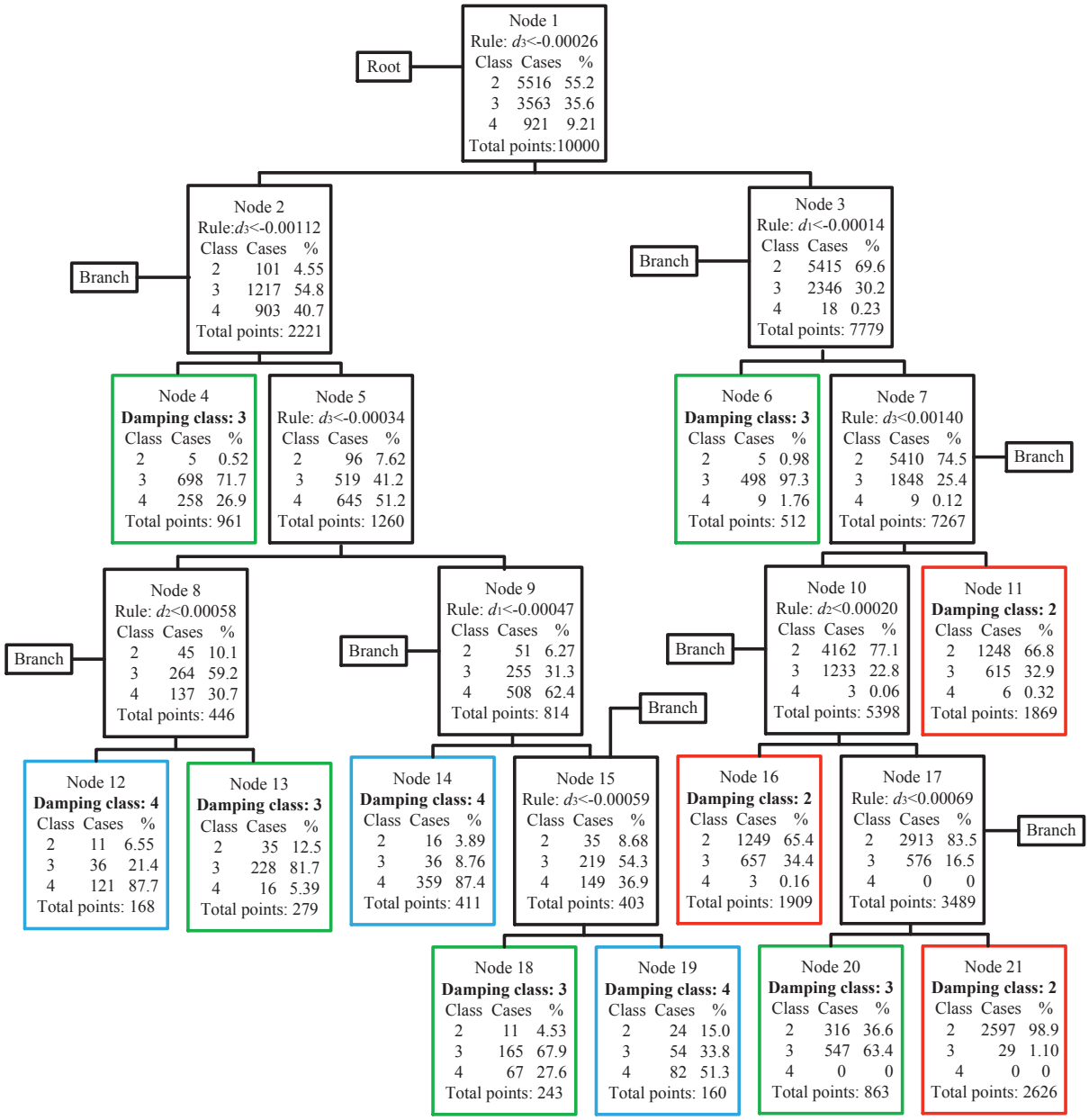

Fig. 6. Decision tree for distinguishing damping classes.

samples obtained from the proposed method are different from that obtained by the Eigen analysis method, the bulk of the results are the same, which demonstrates that the proposed online stability prediction method is effective for predicting the damping classes.

If the current identifying damping class is "Unstable," "Very inadequate" or "Inadequate," then the operators should take some action to remedy the near instability or unstable electromechanical oscillations, such as reschedule the output power of generators or put the damping controller into service.

VI. Conclusion

The use of decision trees to predict multi-mode damping of a power system incorporating renewable energy sources generation with the help of WAMS has been proposed in this paper. Decision trees are employed as a means to handle vast quantities of wide-area information, which involves the mode damping information indicating the stability. DT is built off-line using the learning data and is regressed online for prediction purposes. The simulation results of 16-generator, 68-bus system added with PV and wind power generation demonstrate that the proposed stability prediction method can predict the damping class correctly using the wide-area information from PMUs, and also can suggest optimal course of action for operators to remedy any near instability or unstable electromechanical oscillations even without prior knowledge of varying output of the renewable energy source power.

REFERENCES

[1] B. Pal and B. Chaudhuri, *Robust Control in Power Systems*, New York: Springer, 2005.

[2] P. Kundur, N. J. Balu, and M. G. Lauby, *Power System Stability and Control*, New York: McGraw-Hill, 1994.

[3] J. G. Slootweg and W. L. Kling, "The impact of large scale wind power generation on power system oscillations," *Electric Power Systems Research*, vol. 67, no. 1, pp. 9–20, 2003.

[4] F. Mei and B. C. Pal, "Modelling of doubly-fed induction generator for power system stability study," in *IEEE Power & Energy Society General Meeting*, 2008, pp. 1–8.

[5] D. Gautam and V. Vittal, "Impact of DFIG based wind turbine generators on transient and small signal stability of power systems," in *IEEE Power & Energy Society General Meeting*, 2009, pp. 1–6.

[6] E. Hinrichsen and P. Nolan, "Dynamics and stability of wind turbine generators," *IEEE Transactions on Power Apparatus and Systems*, vol. 101, no. 8, pp. 2640–2648, 1982.

[7] Y. T. Tan and D. S. Kirschen, "Impact on the power system of a large penetration of photovoltaic generation," in *IEEE Power & Energy Society General Meeting*, 2007, pp. 1–8.

[8] Y. T. Tan, D. S. Kirschen, and N. Jenkins, "A model of PV generation suitable for stability analysis," *IEEE Transactions on Energy Conversion*, vol. 19, no. 4, pp. 748–755, 2004.

[9] L. Wang and T. C. Lin, "Dynamic stability and transient responses of multiple grid-connected PV systems," in *IEEE PES T&D Conference*, 2008, pp. 1–6.

[10] N. Uchida and T. Nagao, "A new eigen-analysis method of steady-state stability studies for large power systems: S matrix method," *IEEE Transactions on Power Systems*, vol. 3, no. 2, pp. 706–714, 1988.

[11] D. Lam, H. Yee, and B. Campbell, "An efficient improvement of the AESOPS algorithm for power system eigenvalue calculation," *IEEE Transactions on Power Systems*, vol. 9, no. 4, pp. 1880–1885, 1994.

[12] D. J. Trudnowski, J. M. Johnson, and J. F. Hauer, "Making prony analysis more accurate using multiple signals," *IEEE Transactions on Power Systems*, vol. 14, no. 1, pp. 226–231, 1999.

[13] P. Shea, "A high-resolution spectral analysis algorithm for power-system disturbance monitoring," *IEEE Transactions on Power Systems*, vol. 17, no. 3, pp. 676–680, 2002.

[14] J. Machowski, J. Bialek, and J. Bumby, *Power System Dynamics: Stability and Control*, Oxford, U.K.: Wiley, 2011.

[15] D. Wilson, K. Hay, P. McNabb, J. Bialek, Z. Lubosny, N. Gustavsson, and R. Gudmansson, "Identifying sources of damping issues in the icelandic power system," in *Proceedings of 16th Power Systems Computation Conference*, 2008, pp. 1–8.

[16] A. G. Phadke and J. S. Thorp, *Synchronized Phasor Measurements and Their Applications*, New York: Springer, 2008.

[17] A. G. Phadke, "Synchronized phasor measurements—A historical overview," in *IEEE/PES Transmission and Distribution Conference and Exhibition*, vol. 1, 2002, pp. 476–479.

[18] R. Bansal, "Bibliography on the fuzzy set theory applications in power systems (1994-2001)," *IEEE Transactions on Power Systems*, vol. 18, no. 4, pp. 1291–1299, 2003.

[19] C. W. Liu, M. C. Su, S. S. Tsay, and Y. J. Wang, "Application of a novel fuzzy neural network to real-time transient stability swings prediction based on synchronized phasor measurements," *IEEE Transactions on Power Systems*, vol. 14, no. 2, pp. 685–692, 1999.

[20] Y. Mansour, E. Vaahedi, M. El-Sharkawi *et al.*, "Dynamic security contingency screening and ranking using neural networks," *IEEE Transactions on Neural Networks*, vol. 8, no. 4, pp. 942–950, 1997.

[21] C. Jensen, M. El-Sharkawi, R. J. Marks *et al.*, "Power system security assessment using neural networks: Feature selection using fisher discrimination," *IEEE Transactions on Power Systems*, vol. 16, no. 4, pp. 757–763, 2001.

[22] L. S. Moulin, M. A. El-Sharkawi, and R. J. Marks, "Support vector machines for transient stability analysis of large-scale power systems," *IEEE Transactions on Power Systems*, vol. 19, no. 2, pp. 818–825, 2004.

[23] ——, "Support vector and multilayer perceptron neural networks applied to power systems transient stability analysis with input dimensionality reduction," in *IEEE Power Engineering Society Summer Meeting*, vol. 3, 2002, pp. 1308–1313.

[24] H. Mori, "State-of-the-art overview on data mining in power systems," in *IEEE Power Systems Conference and Exposition*, 2006, pp. 33–34.

[25] K. Sun, S. Likhate, V. Vittal, V. S. Kolluri, and S. Mandal, "An online dynamic security assessment scheme using phasor measurements and decision trees," *IEEE Transactions on Power Systems*, vol. 22, no. 4, pp. 1935–1943, 2007.

[26] Salford Systems, CART. 2008. [Online]. Available: http://www.salford-systems.com/products/cart.

[27] E. E. Bernabeu, J. S. Thorp, and V. Centeno, "Methodology for a security/dependability adaptive protection scheme based on data mining," *IEEE Transactions on Power Delivery*, vol. 27, no. 1, pp. 104–111, 2012.

[28] K. R. Niazi, C. M. Arora, and S. L. Surana, "Power system security evaluation using ANN: feature selection using divergence," *Electric Power Systems Research*, vol. 69, no. 2, pp. 161–167, 2004.

[29] C. Jensen, M. El-Sharkawi, and R. J. Marks, "Power system security assessment using neural networks: feature selection using fisher discrimination," *IEEE Transactions on Power Systems*, vol. 16, no. 4, pp. 757–763, 2001.

[30] D. Vowles, M. Gibbard, and D. Bones, "Testing continuous-monitoring modal-estimation methods: assessment of the QUT energy-based method (QUT version)," The University of Adelaide, Adelaide, South Australia, 2004, Confidential Rep. AIR C00120, 2004.

[31] R. A. Fisher, "The use of multiple measurements in taxonomic problems," *Annals of Eugenics*, vol. 7, no. 2, pp. 179–188, 1936.

[32] G. Rogers, *Power System Oscillations*. MA: Kluwer, 2012.

Tong Wang (S'09) is currently a Post-Doctoral researcher in the School of Electrical and Electronic Engineering, North China Electric Power University, China. She received her B.S. degree and Ph.D. degree from North China Electric Power University, China, in 2007 and 2013, respectively. She was a visiting researcher scholar from 2011 to 2012 in the Bradley Department of Electrical and Computer Engineering, Virginia Polytechnic Institute and State University, USA. Her interests mainly include wide area measurements, and small signal analysis and control.

Tianshu Bi (SM'09) was born in China in 1973. She received the Ph.D. degree from the Department of Electrical and Electronic Engineering, University of Hong Kong, Hong Kong, in 2002.

She is currently a Professor with the North China Electric Power University, Beijing, China. Her research interests include power system protection and control, synchronized phasor measurement technique and its application, and fault diagnosis.

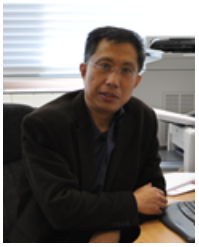

Haifeng Wang (SM'03) was born in 1960 in Jiangsu province. He received his B.S., M.S. and Ph.D. degree from the Department of Electrical and Electronic Engineering, Southeast University, in 1982, 1984 and 1988, respectively. He was a Post-Doctral of Zhejiang University from 1988 to 1989. He was a Research Fellow in the Queen's University of Belfast, Belfast, U.K. from 1990 to 1993. He was Senior Research Fellow in Manchester Metropolitan University, Manchester, U.K. from 1994 to 1997. He was a Senior Lecturer in University of Bath, Bath, U.K. from 1997 to 2007. From 2007 to 2013, he was a Professor of Queen's University of Belfast, Belfast, U.K.

Currently, he is a Professor at the North China Electric Power University, Beijing, China. His main research interests are power system stability analysis and control, including energy storage systems, FACTS, EV, and renewable power generations.

Jizhen Liu was born in Shanxi Province in 1951. He received his bachelors and masters degree from North China Electric Power University in 1977 and 1982 respectively. He is currently a Professor at NCEPU and also serves as the President of the University. He is also the Director of State Key Laboratory of Alternate Electrical Power System with Renewable Energy Sources, Chief Scientist of the 973 Program. He is a Member of Department of Science and Technology, Member of National Electrical Safety Expert Committee, Chairman of the Automation of the Electric Power Industry Standardization Committee, and Fellow of Institution of Engineering and Technology (IET). His research interests are modeling and control of complex systems, measurement and control theory, and technology for industrial processes.